

Macroscale Tribological Properties of Fluorinated Graphene

Kento Matsumura, Shohei Chiashi, Shigeo Maruyama, Junho Choi*

Department of Mechanical Engineering, The University of Tokyo, 7-3-1 Hongo, Bunkyo-ku, Tokyo

113-8656, Japan

*E-mail: choi@mech.t.u-tokyo.ac.jp

Abstract

Because graphene is carbon material and has excellent mechanical characteristics, its use as ultrathin lubrication protective films for machine elements is greatly expected. The durability of graphene strongly depends on the number of layers and the load scale. For use in ultrathin lubrication protective films for machine elements, it is also necessary to maintain low friction and high durability under macroscale loads in the atmosphere. In this study, we modified the surfaces of both monolayer and multilayer graphene by fluorine plasma treatment and examined the friction properties and durability of the fluorinated graphene under macroscale load. The durability of both monolayer and multilayer graphene improved by the surface fluorination owing to the reduction of adhesion forces between the friction interfaces. This occurs because the carbon film containing fluorine is transferred to the friction-mating material, and thus friction acts between the two carbon films containing fluorine. On the other hand, the friction coefficient decreased from 0.20 to 0.15 by the fluorine plasma treatment in the multilayer graphene, whereas it increased from 0.21 to 0.27 in the monolayer graphene. It is considered that, in the monolayer graphene, the change of the surface structure had a stronger influence on the friction coefficient than in the multilayer graphene, and the friction coefficient increased mainly due to the increase in defects on the graphene surface by the fluorine plasma treatment.

Keywords: graphene; fluorination; friction; durability

1. Introduction

Graphene was discovered in 2004 by exfoliating the surface of graphite, and it has since been attracting attention in various research fields. Graphene is the two-dimensional monolayer or multilayer carbon sheets having thicknesses of only several atoms. The carbon atoms are sp^2 -bonded to each other, and thus graphene has excellent chemical stability, thermal conductivity, electronic mobility, transparency, and mechanical strength [1]. It is expected that because of these characteristics, graphene, which has a high fracture strength of approximately 130 GPa and a Young's modulus greater than 1 TPa [2], will be applicable to ultrathin lubricant protective films for machine elements, such as micro-molds, microelectromechanical system (MEMS) devices, and magnetic disks. As for the friction properties of graphene, many studies have been carried out under nanoscale load by means of friction measurements using atomic force microscopy and molecular dynamics simulations, and it has been reported that the more the graphene layers are, the less the friction coefficient of graphene is [3-5]. The application of graphene to ultrathin lubricant protective films could be achieved if low friction is maintained with a smaller number of layers. Furthermore, it is necessary to clarify the friction and durability characteristics of graphene not only under nanoscale load but also under macroscale load in order to use it as lubricant protective films for machine parts, as mentioned earlier.

In order to develop new functionality while maintaining the properties of graphene, modification of graphene with other atoms (e.g., hydrogen, fluorine, nitrogen) using plasma treatment is being vigorously explored [6-10]. Most studies on the friction properties of graphene modified with other atoms are performed under nanoscale load, and it has been reported that the modification of graphene with fluorine makes the graphene surface three-dimensional, thus increasing the friction coefficient [11-15]. On the other hand, as far as the authors know, the friction properties for graphene modified with fluorine atoms under macroscale load have not been reported. Though three-dimensional atomic structure of fluorinated graphene film is critical mechanism for the high friction properties under nanoscale load, it is reasonable to assume that we can achieve low friction under macroscale load by modifying graphene with fluorine because it is well known that low friction is provided by adding fluorine to amorphous carbon films under macroscale load [16-18].

The purpose of this study is therefore to clarify the tribological properties under macroscale load of monolayer and multilayer graphene whose surfaces were modified by fluorine plasma treatment.

2. Experimental

Both monolayer and multilayer graphene were synthesized on Cu foil using thermal chemical vapor deposition (CVD) technique [19]. A mixture of CH_4 and H_2 was used as the source gas. Table 1 and Fig. 1 show, respectively, the conditions and the temperature history of the synthesis of graphene. First, after annealing the Cu foil in a H_2 atmosphere at $1000^\circ C$, graphene was synthesized on the Cu foil by flowing CH_4 gas. Monolayer and multilayer graphene were synthesized both by folding and not folding, respectively, the Cu foil [20]. After the transfer of the synthesized graphene onto the SiO_2 substrate [21], fluorine plasma treatment was performed on the graphene surface using bipolar plasma based ion implantation (bipolar PBII) [22]. The monolayer thickness of the graphene was measured using noncontact mode atomic force microscopy.

Plasma treatment was performed using CF_4 as a source gas, and the conditions are given in Table 2. The fluorinated graphene was evaluated by Raman spectroscopy (wavelength: 532 nm) and X-ray photoelectron spectroscopy (XPS). **The C1s peaks in the XPS spectra were deconvoluted to Lorentz-Gaussian peaks with a Shirley background.** The bipolar PBII method is a technique of ion implantation in which a positive voltage is first applied to the substrate to produce plasma in the peripheral area of substrate, and then ions in the plasma are incident on the negatively biased substrate. Note that the process can also be applied to three-dimensionally shaped structures.

Two kinds of sharp peaks, the G and 2D peaks, appear in the Raman spectrum of graphene [23]. The G peak, which comes from all carbon six-membered ring and chain sp^2 bonds, appears near 1580 cm^{-1} . On the other hand, the 2D peak, which comes from the vibration of the whole sheet structure with the sp^2 bonds of the carbon six-membered ring, appears near 2700 cm^{-1} . The intensity ratio between the 2D and G peaks, $I(2D)/I(G)$, indicates the number of graphene layers: a ratio of over $5/3$ corresponds to a monolayer, a ratio of approximately 1 corresponds to two layers, and a ratio of less than $1/2$ corresponds to three or more layers [24]. Furthermore, the D peak, which comes from the breathing mode of the six-membered ring of graphene, appears near 1350 cm^{-1} , and we can evaluate the defect in graphene from the intensity ratio between the D and G peaks, $I(D)/I(G)$. When graphene is modified with other atoms, including fluorine, sp^2 bond turns to sp^3 bond and the D peak appears. Furthermore, the intensity of the 2D peak decreases in comparison to that of the G peak by the modification with other atoms [6, 25]. It is known that fluorinated graphene returns to the pristine graphene by annealing it in vacuum for 45 minutes at 697°C [6]; thus, we can determine whether the six-membered ring structure of graphene is destroyed by plasma treatment.

The friction properties and durability of graphene before and after the fluorine plasma treatment were studied by means of ball-on-disk-type friction testing. The friction test was performed in the atmosphere with a friction velocity of 60 rpm, a load of 0.98 N, and bearing steel balls (JIS SUJ2, ASTM 52100) 5 mm in diameter as the friction-mating material. Because the friction properties of a carbon-based material strongly depend on the relative humidity [26, 27], the relative humidity was set to 30% by a humidity generator in the friction testing of this study. **The friction coefficients were obtained by averaging the friction coefficients during the stable period before the destruction of graphene.**

3. Results and discussion

3.1 Synthesis and fluorine plasma treatment of graphene

Figures 2(a) and (b) show the Raman spectra of the multilayer and monolayer graphene, respectively, synthesized by thermal CVD. In Fig. 2(a), the number of layers in the multilayer graphene is 2 or 3, as judged from the $I(2D)/I(G)$ ratio [24]. **Figures 3(a) and 3(b) show the AFM image of the boundary between the transferred monolayer graphene sheet and SiO_2 substrate and the measured thickness of the graphene, respectively. The measured thickness of the monolayer graphene was 0.78 nm, which is comparable to the measured thickness of monolayer graphene, 0.9 nm, by Ishigami *et. al.* using AFM in air [28]. These values**

are relatively large compared to the layer-to-layer spacing in bulk graphite, 0.34 nm. Ishigami *et. al.* reported that this discrepancy is attributed to the presence of ambient species between SiO₂ and the graphene sheet.

Figures 4(a) and (b) show the Raman spectra of the multilayer and monolayer graphene, respectively, after the fluorine plasma treatment. The D peak increased and the 2D peak decreased after the fluorine plasma treatment in both the monolayer and multilayer graphene, and these results are resemble those reported by Chen *et al.*, where the fluorine plasma treatment was performed by reactive ion etching [6].

Table 3 shows the surface atomic composition of the multilayer and monolayer graphene after the fluorination as measured by XPS. The results confirm that the surfaces of both the multilayer and monolayer graphene contained a certain amount of fluorine. Because the surfaces contained less fluorine than the theory predicted [29], it is unlikely that the entire surface of the graphene was modified by fluorine. It is worthy to note that the fluorine content of the multilayer graphene is higher than that of the monolayer graphene. One possible reason is that the thickness of monolayer graphene is so thin that the substrate (SiO₂) chemistry is reflected more on the spectrum. In a result, the fluorine content of the monolayer graphene is relatively reduced, while Si and O contents are considerably enhanced. Furthermore, the measured atomic ratio of Si and O in case of the monolayer graphene is about 1:2, which is the composition of SiO₂ substrate. Other possible reason is the increase of defects in the surface of the monolayer graphene by the fluorine plasma treatment. In case of the multilayer graphene, even if the defects are generated on the uppermost surface, the second or the third layer of the graphene sheet is fluorinated.

Figure 5 shows the C1s and F1s peaks of the multilayer graphene after the fluorination. The C1s spectrum contains peaks at binding energies of 285.7, 287.7, 290.0 and 292.5 eV, indicating C-CF, CF, CF₂ and CF₃ bonds [30, 31], respectively and the F1s peak is seen sharply, suggesting the presence of chemical bonds between C and F. In addition, it can be said that the modification with fluorine through the fluorine plasma treatment using CF₄ gas by the PBII technique resulted in a mixture of CF and CF₂ bonds.

Figure 6 shows the change of the Raman spectra of monolayer graphene modified with fluorine after annealing in vacuum for 45 minutes at 700°C. Figure 6(a) shows the spectrum after fluorine plasma treatment and Fig. 6(b) shows the spectrum after the vacuum annealing. Because the D peak decreases and the 2D peak increases through the annealing in vacuum and we can confirm the Raman spectrum of graphene that resembles that of graphene before modification with fluorine, it is clear that the structure of graphene was not destroyed by the plasma treatment. However, the D peak, which indicates graphene defects, was slightly larger than the original D peak of graphene [Fig. 2(b)]; this shows that some defects were created by the plasma treatment.

3.2 Friction and durability properties

Figure 7 shows the results of the friction tests before and after the fluorine plasma treatment of both the monolayer and multilayer graphene. Regarding the durability improvement by the fluorine plasma treatment, the graph shows that the durability of the fluorinated multilayer graphene lasted approximately 10 times longer than that of the untreated multilayer, whereas the durable time of the fluorinated monolayer was approximately

4 times longer than that of the untreated monolayer. Figure 8 shows the Raman spectra of the transfer layer on the steel ball surface, while low friction was maintained in the multilayer graphene before (Fig. 8(a)) and after (Fig. 8(b)) the fluorine plasma treatment. Raman spectroscopy was measured in the central part of the worn surface of the steel ball. From the fact that the sharp D, G, and 2D peaks are observed in both Raman spectra before and after the fluorine plasma treatment, it is understood that the transfer layer was an amorphous carbon film with a graphene structure. Table 4 presents the XPS results, showing the change in the atomic composition of the wear track in the fluorinated multilayer graphene. These were measured before the friction test and after sliding of 350 and 600 cycles (refer to Fig. 7(c)). Although the fluorine content of the graphene surface decreased through the friction test, fluorine was still observed on the sliding surface when low friction was sustained at the 350 cycles. As shown in Fig. 6, because fluorinated graphene was transferred to the steel ball surface and then the sliding occurred between the fluorinated graphene and the transfer layer that is the mixed structure of the fluorinated amorphous carbon and fluorinated graphene, a low friction could be achieved.

Jaoul et al. performed friction experiments in a dry environment between fluorinated amorphous carbon films and a steel ball (100Cr6 steel) surface. They reported that the durability of the film improved and the friction coefficient decreased by adding fluorine [16]. In addition, Rubio-Roy et al. performed friction experiments between fluorinated amorphous carbon films and tungsten carbide balls in a N_2+H_2O environment and reported that the incorporation of fluorine was chemically beneficial (that is, there was a decrease of surface free energy and passivation of carbon with high-energy bonds) [17]. Also in our study, it is considered that as the mixture of fluorinated graphene and fluorinated amorphous carbon was transferred to the steel ball surface, the surface energy decreased, similar to the friction behavior of the fluorinated amorphous carbon film, and the decrease of the adhesion between the friction surfaces led to high durability.

As for the friction properties, the friction coefficient decreased from 0.20 to 0.15 by the fluorine plasma treatment in the multilayer graphene, whereas it increased from 0.21 to 0.27 in the monolayer graphene. In the case of multilayer graphene, similar to the friction behavior that contributed to the durability, the fluorinated carbon film was transferred onto the steel ball surface. Friction acted between the carbon films with terminating fluorine atoms, and the friction coefficient decreased because of the decrease of the adhesion force between the friction surfaces. In the case of monolayer graphene, it is thought that the change of surface structure had a somewhat greater influence on the friction coefficient in comparison to the case for multilayer graphene. As shown in Fig. 4, some quantity of defects indicated by the D peak remained, after the annealing in vacuum. Also in the study of Chen et al. [6], the D peak was greater in the graphene annealed in vacuum after the fluorination as compared to the graphene before the modification with fluorine. It is likely that the increase of the friction coefficient of monolayer graphene was mainly due to the increase of defects in the surface by the fluorine plasma treatment. In the case of multilayer graphene, even if defects remained on the uppermost surface, the second or the third layer of the graphene sheet maintained low friction.

4. Conclusions

Through fluorine plasma treatment of the surfaces of both monolayer and multilayer graphene, we studied the friction properties of the fluorinated graphene under macroscale load. The obtained conclusions are as follows:

- (1) The multilayer and monolayer graphene surfaces were successfully modified with fluorine using the bipolar PBII.
- (2) In multilayer and monolayer graphene, a transfer layer, which had a mixture of fluorinated graphene and amorphous carbon, was built up in the friction interface by the fluorine plasma treatment. As a result, the surface energy decreased and the durability of the graphene improved. In addition, the increase in the durability by fluorine plasma treatment was greater in the multilayer graphene.
- (3) In the multilayer graphene, the friction coefficient decreased because the surface energy (adhesion) in the friction interface decreased as a result of the fluorine plasma treatment. On the other hand, in the monolayer graphene, the change of the surface structure influenced the friction properties more strongly in comparison to the multilayer graphene, and the main cause of the increase of the friction coefficient was likely due to the increase of defects in the monolayer graphene surface by the fluorine plasma treatment.

Acknowledgements

This work was supported by KAKENHI (26289024). The authors are grateful to Dr. Jongduk Kim and Mr. Lijing Qui of Park Systems Japan Inc. for the AFM observation.

References

- [1] V. Singh, D. Joung, L. Zhai, S. Das, S. I. Khondaker, S. Seal, *Prog. Mater. Sci.* 56 (2011) 1178-1271.
- [2] C. Lee, X. Wei, J. W. Kysar, J. Hone, *Science* 321 (2008) 385-388.
- [3] T. Filleter, J. L. McChesney, A. Bostwick, E. Rotenberg, K. V. Emtsev, Th. Seyller, K. Horn, R. Bennewitz, *Phys. Rev. Lett.* 102 (2009) 086102.
- [4] Q. Li, C. Lee, R. W. Carpick, J. Hone, *Phys. Status Solidi B* 247 (2010) 2909-2914.
- [5] C. Lee, Q. Li, W. Kalb, X. Z. Liu, H. Berger, R. W. Carpick, J. Hone, *Science* 328 (2010) 76-80.
- [6] M. Chen, H. Zhou, C. Qiu, H. Yang, F. Yu, L. Sun, *Nanotechnology* 23 (2012) 1-6.
- [7] J. T. Robinson, J. S. Burgess, C. E. Junkermeier, S. C. Badescu, T. L. Reinecke, F. K. Perkins, M. K. Zalalutdniov, J. W. Baldwin, J. C. Culbertson, P. E. Sheehan, E. S. Snow, *Nano Lett.* 10 (2010) 3001-3005.
- [8] B. Eren, D. Hug, L. Marot, R. Pawlak, M. Kisiel, R. Steiner, D. M. Zumbühl, E. Meyer, *Beilstein J. Nanotechnol.* 3 (2012) 852-859.
- [9] D. C. Elias, R. R. Nair, T. M. G. Mohiuddin, S. V. Morozov, P. Blake, M. P. Halsall, A. C. Ferrari, D. W. Boukhvalov, M. I. Katsnelson, A. K. Geim, K. S. Novoselov, *Science* 323 (2009) 610-613.
- [10] A. L. Friedman, C. D. Cress, S. W. Schmucker, J. T. Robinson, O. M. J. Erve, *Phys. Rev. B* 93 (2016) 161409 1-10.
- [11] S. Kwon, J. Ko, K. Jeon, Y. Kim, J. Park, *Nano Lett.* 12 (2012) 6043-6048.
- [12] Y. Dong, X. Wu, A. Martini, *Nanotechnology* 24 (2013) 375701.
- [13] Q. Li, X. Liu, S. Kim, V. B. Shenoy, P. E. Sheehan, J. T. Robinson, R. W. Carpick, *Nano Lett.* 14 (2014) 5212-5217.
- [14] J. Wang, F. Wang, J. Li, S. Wang, Y. Song, Q. Sun, Y. Jia, *Tribol. Lett.* 48 (2012) 255-261.
- [15] G. Fessler, B. Eren, U. Gysin, T. Glatzel, E. Meyer, *Appl. Phys. Lett.* 104 (2014) 041910.
- [16] C. Jaoul, C. Dublanche-Tixier, O. Jarry, P. Tristant, J.P. Lavoute, L. Kilman, M. Colas, E. Laborde, H. Ageorges, *Surf. Coat. Technol.* 237 (2013) 328-332.

- [17] M. Rubio-Roy, C. Corbella, E. Bertran, S. Portal, M.C. Polo, E. Pascual, J.L. Andújar, *Diamond. Relat. Mater.* 18 (2009) 923-926.
- [18] C. Donnet, J. Fontaine, A. Grill, V. Patel, C. Jahnes, M. Belin, *Surf. Coat. Technol.* 94-95 (1997) 531-536.
- [19] S. Mikhailov (Ed.), *Physics and Applications of Graphene – Experiments*, InTech, 2011, 37-54.
- [20] X. Li, C. W. Magnuson, A. Venugopal, R. M. Tromp, J. B. Hannon, E. M. Vogel, L. Colombo, R. S. Ruoff, *J. Am. Chem. Soc.* 133 (2011) 2816-2819.
- [21] J. W. Suk, A. Kitt, C. W. Magnuson, Y. Hao, S. Ahmed, J. An, A. K. Swan, B. B. Goldberg, R. S. Ruoff, *ACS Nano.* 5 (2011) 6916–6924.
- [22] S. Miyagawa, S. Nakao, M. Ikeyama, Y. Miyagawa, *Surf. Coat. Technol.* 156 (2002) 322-327.
- [23] A. C. Ferrari, J. C. Meyer, V. Scardaci, C. Casiraghi, M. Lazzeri, F. Mauri, S. Piscanec, D. Jiang, K. S. Novoselov, S. Roth, A. K. Geimet. al., *Phys. Rev. Lett.* 97 (2006) 187401.
- [24] M. S. Dresselhaus, A. Jorio, M. Hofmann, G. Dresselhaus, R. Saito, *Nano Lett.* 10 (2010) 751-758.
- [25] Z. Luo, T. Yu, K. Kim, Z. Ni, Y. You, S. Lim, Z. Shen, S. Wang, J. Lin, *ACS Nano* 3 (2009) 1781-1788.
- [26] S. Bhowmick, A. Banerji, A. T. Alpas, *Carbon* 87 (2015) 374-384.
- [27] A. Banerji, S. Bhowmick, M.J. Lukitsch, A.T. Alpas, *MRS Proceedings* 1812 (2016) 8pp.
- [28] M. Ishigami, J. H. Chen, W. G. Cullen, M. S. Fuhrer, E. D. Williams, *Nano Lett.* 7 (2007) 1643-1648.
- [29] M. Pumera, C. H. A. Wong, *Chem. Soc. Rev.* 42 (2013) 5987-5995.
- [30] K. Hou, P. Gong, J. Wang, Z. Yang, Z. Wang, S. Yang, *RSC Adv.* 4 (2014) 56543-56551.
- [31] X. Wang, Y. Dai, J. Gao, J. Huang, B. Li, C. Fan, J. Yang, X. Liu, *ACS Appl. Mater. Inter.* 5 (2013) 8294-8299.

Figure captions

Fig. 1 Temperature history of graphene synthesis using thermal CVD.

Fig. 2 Raman spectra of graphene: (a) multilayer graphene and (b) monolayer graphene.

Fig. 3 (a) Noncontact mode AFM image of the boundary between the transferred monolayer graphene and SiO₂ substrate and (b) the measured thickness of the graphene.

Fig. 4 Raman spectra of graphene: (a) fluorinated multilayer graphene and (b) fluorinated monolayer graphene.

Fig. 5 XPS (a) C1s and (b) F1s peaks of fluorinated multilayer graphene.

Fig. 6 Raman spectra of (a) the fluorinated monolayer graphene and (b) after the vacuum annealing of the fluorinated monolayer graphene by thermal treatment.

Fig. 7 Friction coefficients of (a) multilayer graphene, (b) monolayer graphene, (c) fluorinated multilayer graphene, and (d) fluorinated monolayer graphene.

Fig. 8 Raman spectra of the transfer films on the steel balls (a) before the fluorination and (b) after the fluorination (inset: optical microscope images of the transfer films).

Table 1 Conditions of graphene synthesis by thermal CVD.

Thickness of copper foil		25 μm
Annealing of Cu foil	Precursor gas	H_2
	Temperature	1000 $^\circ\text{C}$
	Time	40 min
	Pressure	65 Pa
Synthesis of graphene	Precursor gas	A mixture of CH_4 and H_2
	Temperature	1000 $^\circ\text{C}$
	Time	60 min
	Pressure	130 Pa

Table 2 Conditions of fluorine plasma treatment by PBII.

Precursor gas	CF_4
Pulse frequency	1000 Hz
Positive pulse voltage	1.5 kV
Negative pulse voltage	-0.5 kV
Treatment pressure	0.4 Pa
Treatment time	5 s

Table 3 Composition (at.%) of fluorinated graphene surface measured by XPS.

	C	O	F	Si
Multilayer graphene	56.3	16.2	24.0	3.5
Monolayer graphene	58.4	25.9	6.2	9.5
Theoretical value	66.7	-	33.3	-

Table 4 Composition (at.%) of the wear track in the fluorinated multilayer graphene surface.

	C	O	F	Si	Fe
Before sliding	56.3	16.2	24.0	3.5	0
After 350 cycles	60.9	29.6	6.0	2.4	1.1
After 600 cycles	10.9	55.0	1.1	31.9	1.1

Figure

[Click here to download Figure: Fig-final.pptx](#)

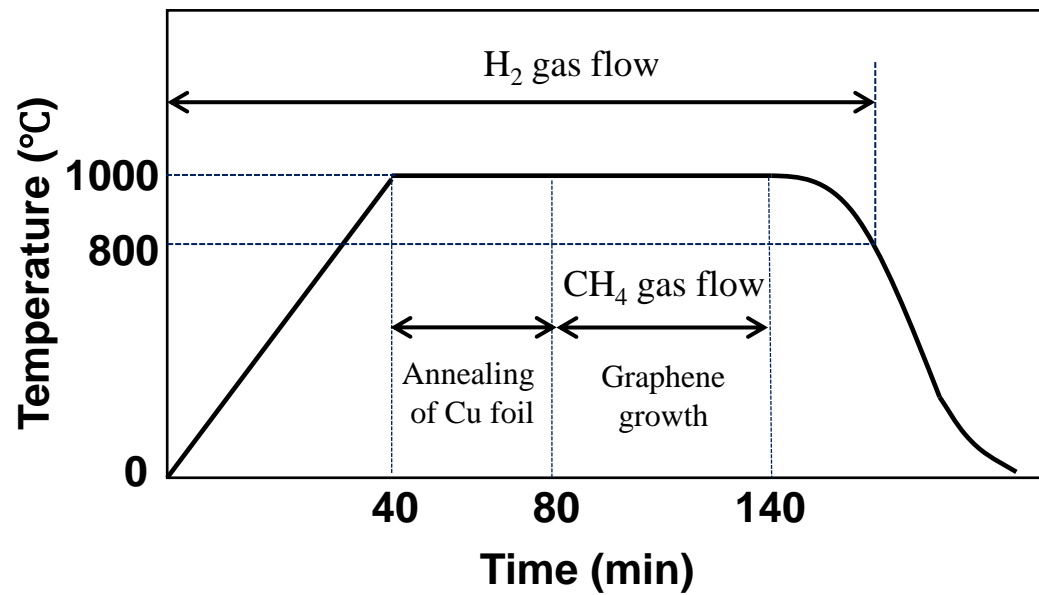


Fig.1

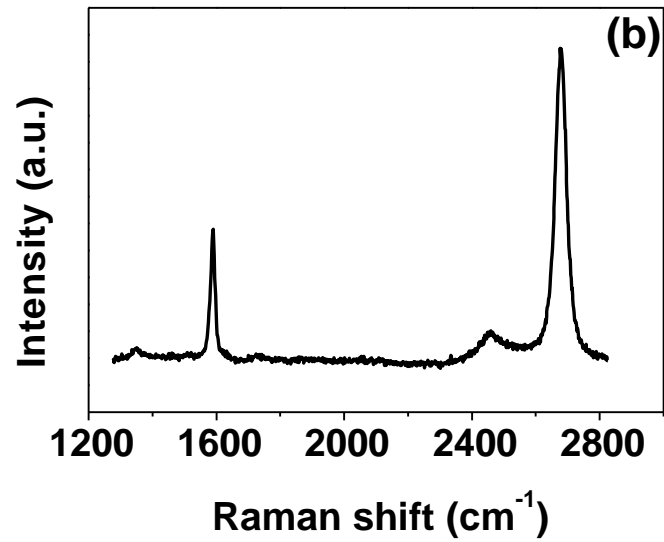
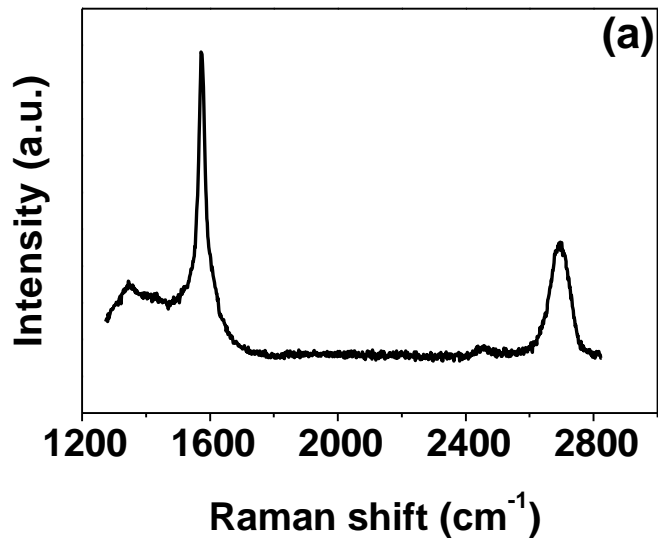


Fig.2

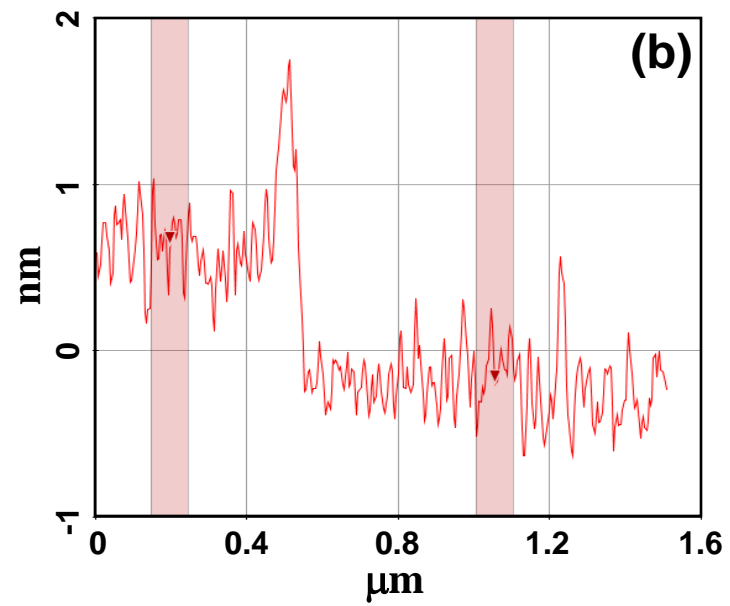
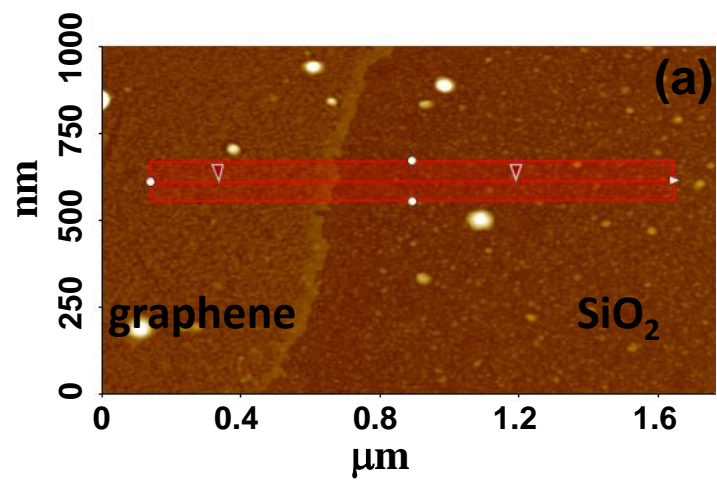


Fig.3

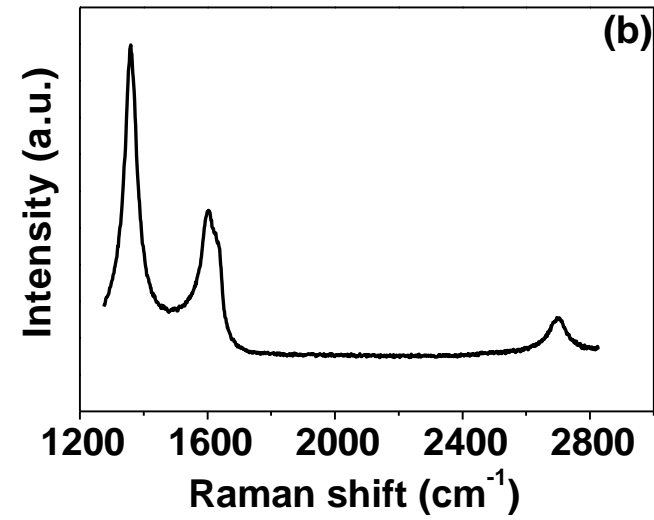
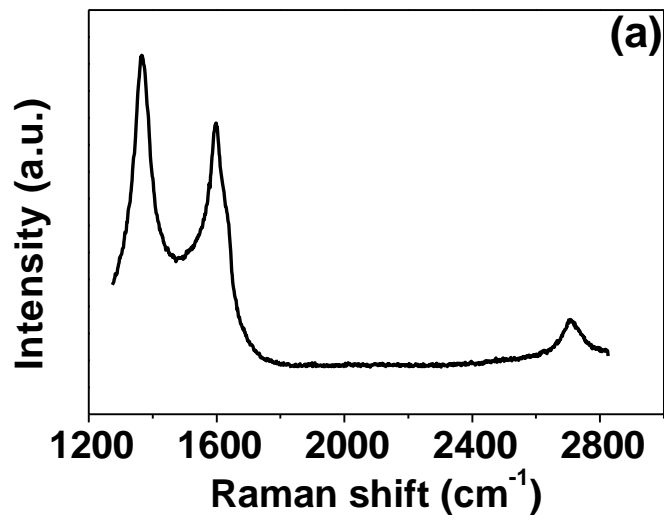


Fig.4

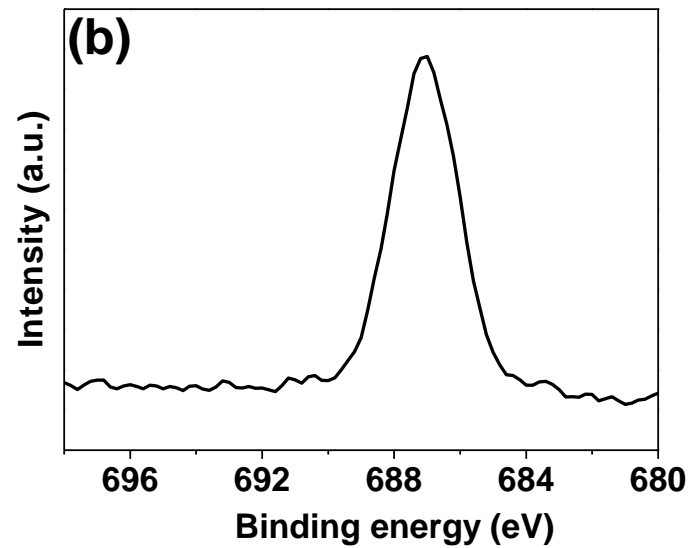
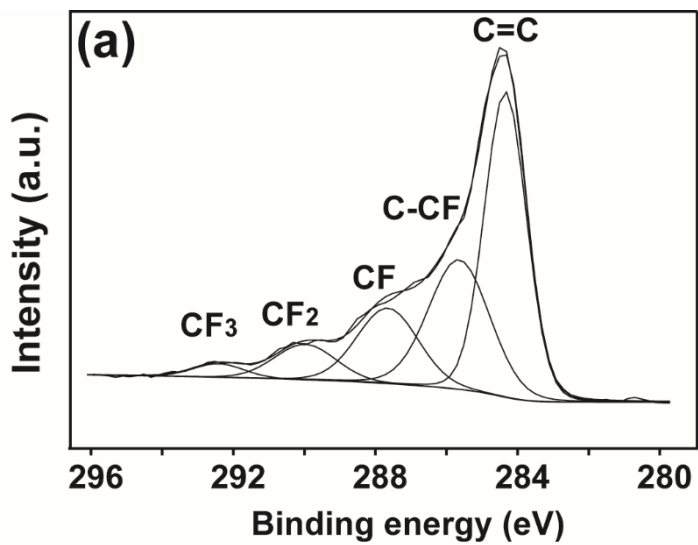


Fig.5

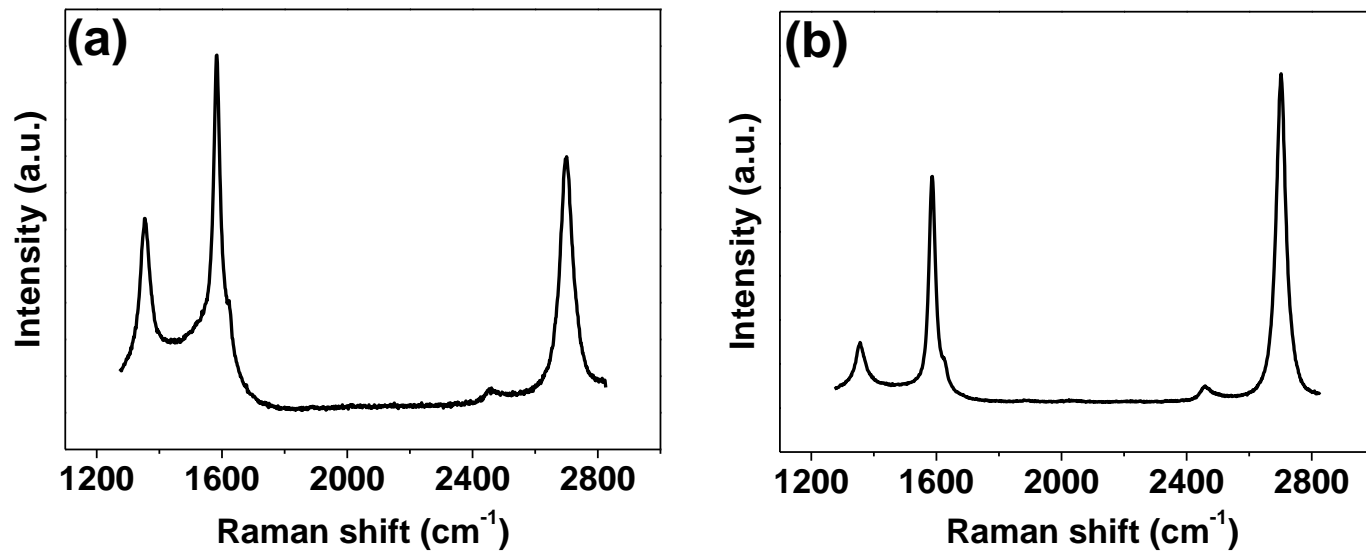


Fig.6

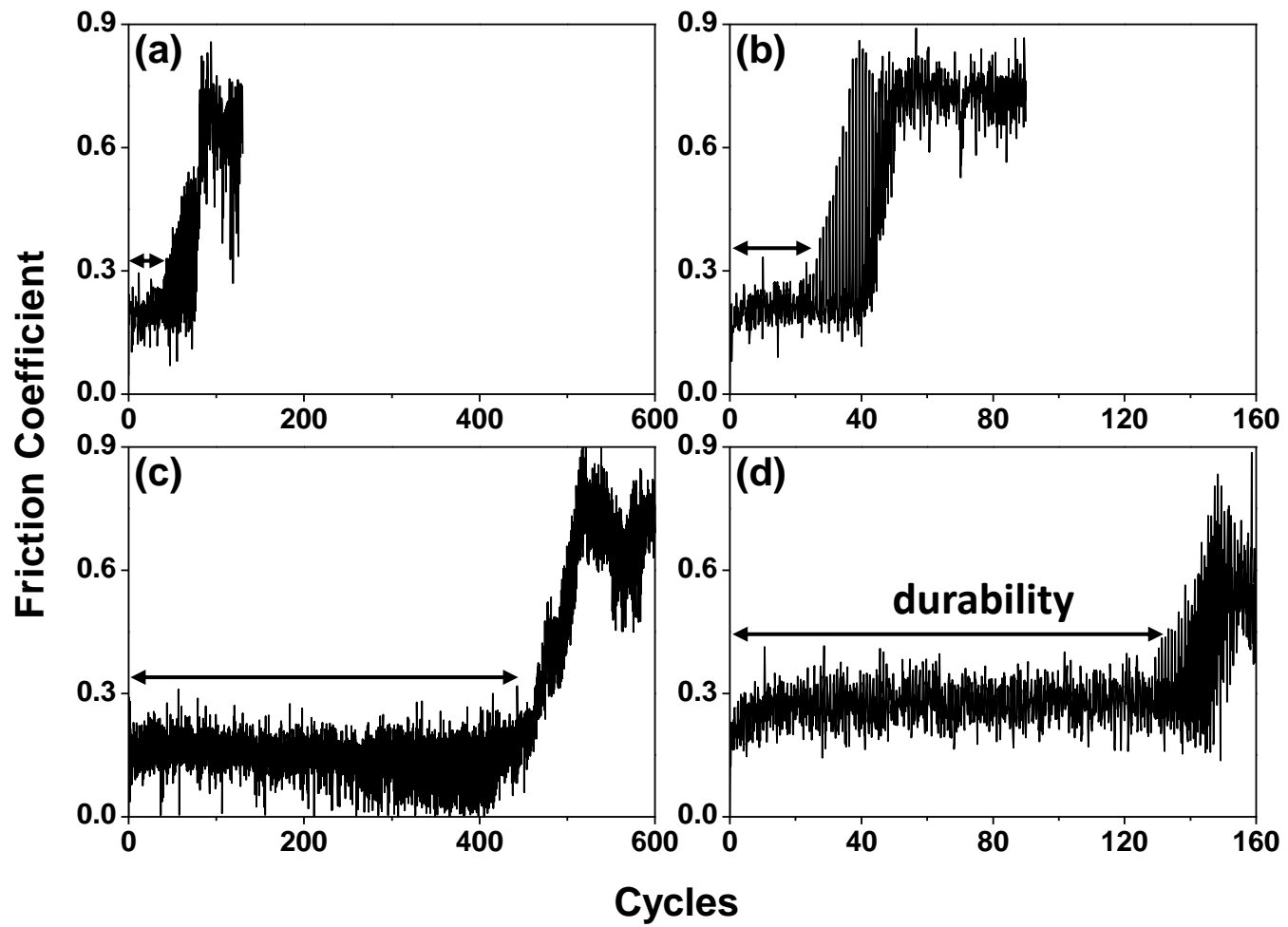


Fig.7

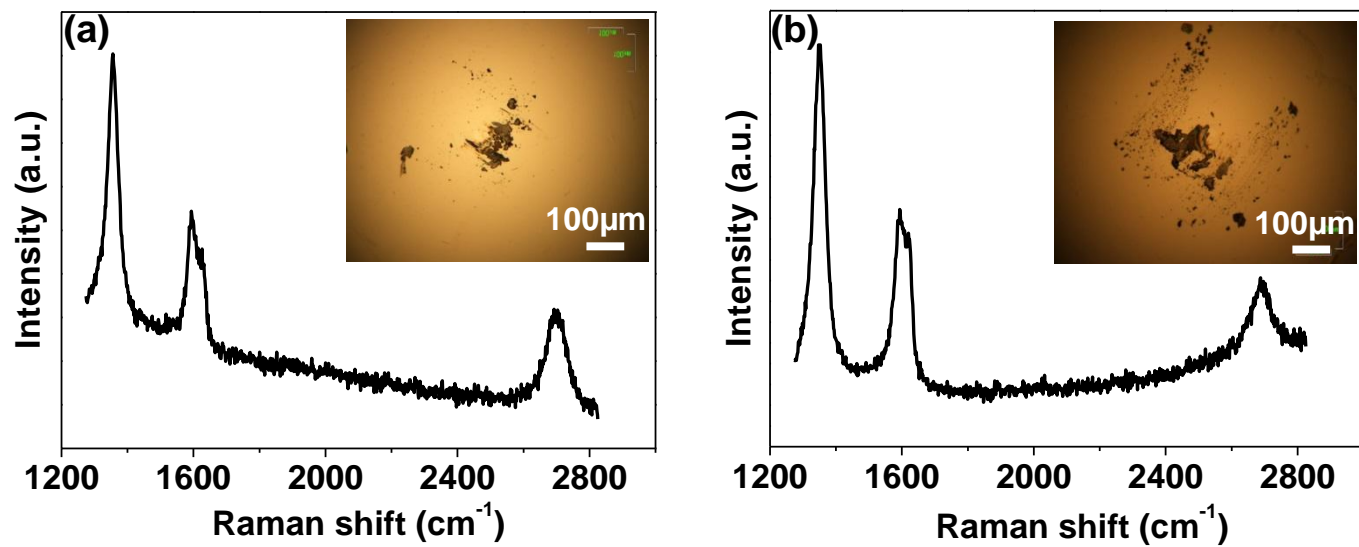


Fig.8